THE ATTENUATION OF STRUCTURAL UPLIFT, WITH DEPTH, BENEATH IMPACT STRUCTURES

Ross W. K. Potter[1,2], David A. Kring[1,2] and Gareth S. Collins[3], [1]Center for Lunar Science and Exploration, Lunar and Planetary Institute, 3600 Bay Area Boulevard, Houston, TX, 77058, USA, [2]NASA Lunar Science Institute, potter@lpi.usra.edu; [3]Department of Earth Science and Engineering, Imperial College London, London, SW7 2AZ, UK

Introduction: Structural uplift of target material beneath impact structures is well documented in both terrestrial impacts [1,2] and laboratory experiments [3]. The amount of structural uplift has been estimated as approximately one-tenth of the final crater diameter for terrestrial [1,2,4] and lunar [5] craters. These estimates, however, are derived from relatively small complex craters that may not be good proxies for impact basins. Those estimates also only refer to lithologies at, or near, the surface. Seismic studies beneath Chicxulub [6,7] and numerical modeling of large-scale impact events [8,9] suggest structural uplift attenuates with depth beneath the crater floor. In this work, we model large basin-scale impact events to produce a set of simple equations that can be used to calculate the maximum amount of structural uplift and its attenuation with depth beneath basins on the Moon.

Methods: We use the iSALE 2D [10-12] shock physics code, previously used to model large-scale impact events (e.g., Chicxulub [8]; South Pole-Aitken [13]), to simulate lunar basin-forming impacts. An infinite half-space target was divided into a crustal (60 km thick) and mantle layer, each of which had properties appropriate for their lunar counterparts [14-17]. A Tillotson equation of state for gabboric anorthosite [18] represented the crustal response to thermodynamic changes and compressibility; ANEOS equations of state tables for dunite [19] were used for the mantle and impactor.

Two thermal profiles based on estimates of ~4 Ga lunar temperature-depth profiles [20,13] were used. Both profiles had similar crustal temperature gradients (10 K/km). In the mantle, temperatures were at the solidus between depths of 150-350 km and ~1670 K below 800 km in thermal profile 1; in thermal profile 2, mantle temperatures remained sub-solidus and reached temperatures of ~1770 K in the deep mantle. Based on the thermal profiles, self-consistent pressure, density and strength fields were computed. The gravity field was kept constant at 1.62 m/s^2. Impactor diameter was varied between 40 and 120 km (though the number of cells across the impactor was constantly 40); impact velocity varied between 10 and 20 km/s.

The amount of structural uplift achieved during basin formation was quantified using Lagrangian tracer particles. These tracer particles, initially placed in every grid cell and assigned to a mass of material, tracked the location of that cell material throughout the basin-forming process. Uplift was calculated by comparing the difference in depth along a given row of tracers inside (at the center) and outside the basin.

Results: Figure 1 shows target material distribution following a typical lunar basin-forming impact. Overlaid on the material plot is the grid of Lagrangian tracers (black lines). Crust has been removed from the basin center and mantle uplifted towards the basin floor. The three colored tracer rows highlight the relative changes in uplift between materials from different target depths.

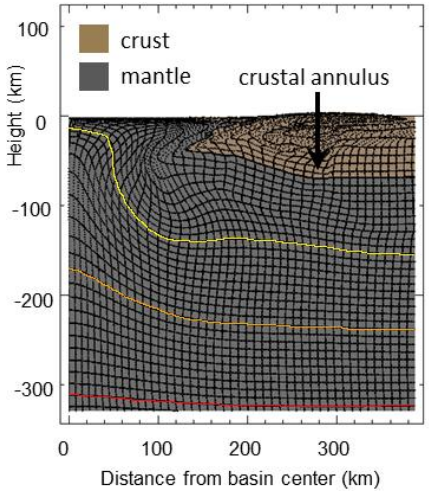

Figure 1: A typical lunar basin model post-impact. Black lines represent tracer particle rows and columns. Colored rows illustrate how uplift varies with depth.

Figure 2 plots maximum structural uplift (U_{max}) against crustal annulus radius (r_{ca}) - the radial distance to the thickest point in the crust (see Figure 1) and an alternative basin size constraint [21] – for the suite of modeled impact scenarios. The data show maximum uplift increases with crustal annulus radius. Results for thermal profile 1 (TP1) and thermal profile 2 (TP2) are fit, respectively, by the equations:

$$U_{max} = 0.45\, r_{ca} \qquad (1)$$

$$U_{max} = 0.56\, r_{ca} \qquad (2)$$

Figure 3a plots structural uplift (U) against depth below the basin floor for a range of modeled lunar basins. Our models suggest uplift reaches a maximum within the upper tens of kilometers of the target rather

than at the target surface. The same data set is plotted logarithmically in Figure 3b highlighting the attenuation of structural uplift with depth. The complete dataset in Figure 3b can be fit reasonably by the equation

$$U = (-0.47 \pm 0.06)z + b \qquad (3)$$

where z is depth below the basin floor and b is ~U_{max}.

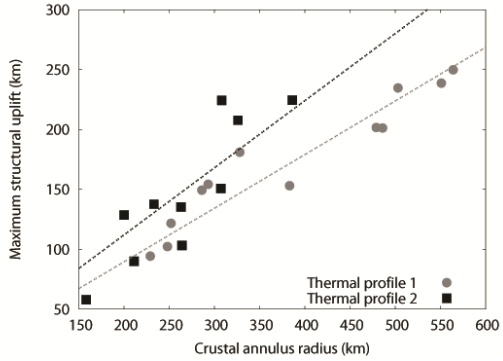

Figure 2: Maximum structural uplift against crustal annulus radius for lunar basin-scale impacts.

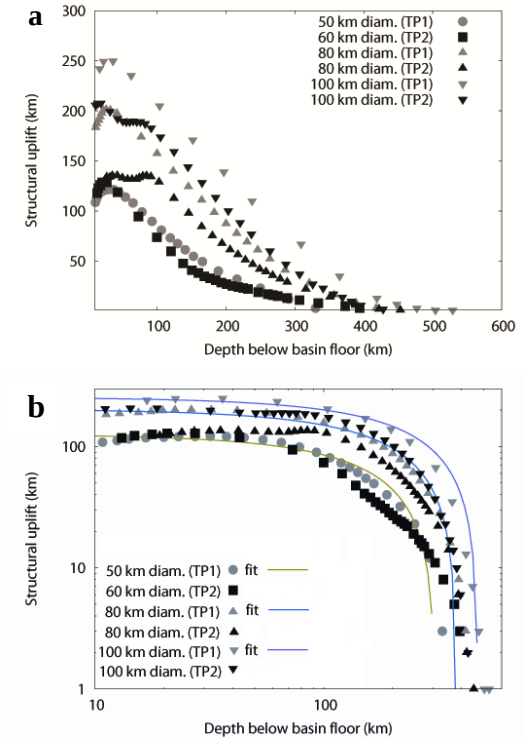

Figure 3: Structural uplift versus depth below basin floor for a suite of modeled lunar basins.

If the crust is slightly thinner (e.g., 40 km as implied by new GRAIL data [22]), these results are not significantly affected.

Discussion: Equations 1 and 2 predict U_{max} to be approximately half the crustal annulus radius, which is itself approximately two-thirds of the final crater radius for lunar basins [23]. U_{max} is, therefore, approximately one-sixth of the final crater diameter for lunar basins. This U_{max} value is two to three times smaller than those estimated for lunar basins using the equation of [5]. That previous work, however, was based on much smaller complex craters and may not extrapolate well to the large impact basins considered here.

Our results indicate structural uplift in the lunar basin centers attenuates with depth, which is qualitatively similar to that seen in numerical models of the terrestrial Chicxulub impact [8]. Importantly, however, Figure 3 and Equation 3 provide, for the first time, constraints on the rate and nature of that attenuation. The model results also show that maximum structural uplift does not occur at the surface. This is due to the outward collapse of the central uplift. If that trend is observed in nature, this may help distinguish between competing models for the formation of large impact basins.

Acknowledgments: We thank Boris Ivanov, Jay Melosh, Kai Wünnemann and Dirk Elbeshausen for their work developing iSALE.

References: [1] Grieve, R. A. F. et al. (1981) *Proc. LPSC 12a*, 37-57 [2] Grieve, R. A. F. and Pilkington, M. (1996) *J. Aus. Geol. Geophys*., 16, 399-420 [3] Schmidt, R. M. and Housen, K. (*1987) Int. J. Impact Eng*., 5, 543-560 [4] Ivanov, B. A. et al. (1982) *Meteoritika*, 40, 67-81[5] Cintala, M. J. and Grieve, R. A. F. (1998) *MAPS*, 33, 889-912 [6] Christeson, G. L. et al. (2001) *JGR*, 106, 21751-21769 [7] Christeson, G. L. et al. (2009) *EPSL*, 284, 249-257 [8] Collins, G. S. et al. (2002) *Icarus*, 157, 24-33 [9] Ivanov, B. A. (2005) *Sol. Sys. Res*., 39, 381-409 [10] Amsden, A. A. et al. (1980) Los Alamos Nat. Lab. Report LA-8095 [11] Collins, G. S. et al. (2004) *MAPS*, 39, 217-231 [12] Wünnemann, K. et al. (2006) *Icarus*, 180, 514-527 [13] Potter, R. W. K. et al. (2012) *Icarus*, 220, 730-743[14] Azmon, E. (1967) NSL 67-224 [15] Stesky, R. M. et al. (1974) *Tectonophys*., 23, 177-203 [16] Shimada, M. et al. (1983) *Tectonophys*., 96, 159-192 [17] Ismail, I. A. H. and Murrell, S. A. F. (1990) *Tectonophys*., 175, 237-248 [18] Ahrens, T. J. and O'Keefe, J. D. (1977) In: Impact and explosion cratering, Pergamon, New York, 639-656 [19] Benz, W. et al. (1989) *Icarus*, 81, 113-131 [20] Spohn, T. et al (2001) *Icarus*, 149, 54-65 [21] Potter, R. W. K. et al. (2012) *GRL*, 39, L18203 [22] Wieczorek, M. A. et al. (2012) *Science*, doi:10.1126/science.1231530 [23] Potter, R. W. K. (2012) Ph.D. Thesis, Imperial College London.